

Spectral Spatial Fluctuations of CMBR: Strategy and Concept of the Experiment

Viktor Dubrovich

*Special Astrophysical Observatory RAS, Pulkovskoe Chaussee 65, St.Petersburg,
Russia*

Anisa Bajkova

*Main Astronomical Observatory RAS, Pulkovskoe Chaussee 65/1, St.Petersburg,
Russia*

V.B.Khaikin

*Special Astrophysical Observatory RAS, Pulkovskoe Chaussee 65, St.Petersburg,
Russia*

Abstract

Spectral Spatial Fluctuations (SSF) of the Cosmic Microwave Background Radiation (CMBR) temperature are considered as a result of an interaction of primordial atoms and molecules with CMBR in proto-objects moving with peculiar velocities relative to the CMBR. Expected optimistic values of $\Delta T/T$ are $2 \times 10^{-5} - 2 \times 10^{-6}$ for SSF caused by HeH^+ at $z = 20-30$ which are possible redshifts of early reionization scenario. The bandwidth of the lines is 0.1-2% depending on the scale of proto-objects and redshifts. For the SSF search CMBR maps in different spectral channels are to be observed and then processed by the Difference method. Simulation of the experiment is made for MSRT (Tuorla Observatory, Finland) equipped with a 7×4 beam cryo-microbolometer array with a chopping flat and frequency multiplexer providing up to 7 spectral channels in each beam (88-100 GHz). Expected $\Delta T/T$ limit in the experiment is 2×10^{-5} with 6'-7' angular and 2% frequency resolution. Simulation shows that SSF may be recognized in the angular power spectrum when S/N in single frequency CMBR maps is as small as 1.17 or even something less for white noise. Such an experiment gives us a possibility to set upper limit of SSF in MM band and prepare future SSF observations.

Key words: Cosmic Microwave Background (CMB), Cosmology, molecules, Radio Telescope

PACS: 98.80.-k, 34.50.-s, 95.85.Bh

1 Introduction

Observational effects caused by primordial molecules seem to be most promising in investigating Dark Ages epoch of the Universe. The basic properties of the molecules are discrete narrow energy levels and high efficiency of their interaction with CMBR. This leads to forming SSF if proto-objects, containing these molecules, move with peculiar velocities V_p relative to CMBR (Dubrovich,1977,1982, Puy,1993). We may consider SSF as manifestation of the proto-objects at high redshifts $300 > z > 10$ as scattering of CMB photons by primordial molecules must leave imprints on the CMBR temperature distribution.

The most abundant chemical elements predicted by the pure Big Bang model are H, He, D, ^3He , Li and their ions. They give some molecules in the primordial matter at $z=100-200$ such as $\text{H}_2, \text{H}_2^+, \text{HD}, \text{HD}^+, \text{HeH}^+, \text{LiH}, \text{LiH}^+, \text{H}_2\text{D}^+$. There are other molecules which should be considered if non-standard nuclear synthesis at the early times ($z=10^9$) or star formation at $z = 100-200$ took place.

For the high efficiency of interaction between molecules and CMBR photons two values are important - the cross-section for scattering and the concentration (or relative abundance) of this molecule. The first parameter depends on the specific quantum structure of the molecule - its symmetry and dipole moment. The second one depends on the abundance of the chemical elements of which it is composed and on the rate of the appropriate chemical reactions. According to these constraints, we should take into consideration only those molecules which have a large enough dipole moment and relatively high abundance. These are $\text{HD}^+, \text{HeH}^+, \text{LiH}, \text{H}_2 \text{D}^+$. We consider them as the basic molecules interacting with CMBR at high z (Dubrovich,1977,1982,Puy et al.,1993,Stancil et al.,1996).

2 Theoretical predictions of SSF

Let us remind physical conditions in Dark Ages epoch when the Universe was younger than 300 mil. years. The Universe was in $(z+1)^{3/2}$ times smaller and in $(z+1)^3$ times more dense than now, temperature of CMBR and molecular gas followed $T_{z=0}(z+1)$ law till $z \approx 150$. Then, temperature of matter should be lower than CMBR temperature due to different adiabatic indexes of radiation and matter (Varshalovich, Hhersonskii, Sunyaev, 1981) and it must

Email addresses: `dubr@MD1381.spb.edu` (Viktor Dubrovich),
`bajkova@gao.spb.ru` (Anisa Bajkova), `vkh@brown.nord.nw.ru` (V.B.Khaikin).

Table 1

Temperatures of CMBR and molecular gas in Dark Ages epoch $z=300-10$

z	Temperature of CMBR, K	Temperature of molecular gas, K	Commentary
1100	3000	3000	Recombination
300	815	815	Beginning of Dark Ages
150	415	415	Middle of Dark Ages
30	85	17	Dark Ages + reionization
20	57	8	Dark Ages + reionization
10	30	100-10000	End of Dark Ages, first stars and quasars

follow $T_{z=0}(z + 1)^2$ law till first star formation. Calculated temperatures of CMBR and molecular gas in Dark Ages epoch are given in Table 1, we used $T_{z=0} = 2.726$ K (Mather et al., 1994). In epoch before secondary ionization molecules are formed in accordance with kinetic rate of specific chemical reactions when matter and radiation are cooling. After reionization molecular formation follows a more complicated law due to growth of ionization degree of hydrogen and existence of heavy chemical elements produced by first stars (Basu, Hernandez-Monteagudo, Sunyaev, 2004).

There are two mechanisms responsible for SSF formation: simple scattering (Dubrovich,1977) and luminescence (Dubrovich,1997). In the simple mechanism opacity in narrow molecular lines and peculiar motion of the proto-clouds results in CMBR disturbances. This can be more visible in the rest frame of the proto-object. The CMBR in this frame becomes non-isotropic and out of thermal equilibrium. On the side towards which the proto-cloud moves, the temperature of the CMBR will be higher than average and on the opposite side it will be lower. After reflection, the photons are distributed isotropically in this frame that leads to non-isotropic distribution in laboratory frame. This explains the principal role of opacity and peculiar velocity. The amplitude of the effect depends on spectral index of the reflecting radiation (Dubrovich, 1977, Maoli et al., 1994). This effect corresponds to the elastic scattering between the molecules and photons, i.e. the total number of the photons does not change.

In fact all molecules have quite a complicated energy level structure. This allows for the possibility of a non-elastic process. It is the well known luminescence process which plays an important role in the formation of radiation from a reflection nebula. Luminescence may enhance the intensity of rotation lines due to breaking of vibrational line quants (Dubrovich, 1997).

The magnitude of the CMBR temperature fluctuations due to the pure reflection of photons by a moving object depends on peculiar velocity V_p of a proto-object and optical depth τ (Sunyaev and Zel'dovich, 1970, Dubrovich, 1977, Maoli et al., 1994). The value of the distortions produced by molecules in CMBR is:

$$\Delta T/T = (V_p/c) \cdot \tau \cdot K, \quad (1)$$

where c is the speed of light and τ is optical depth of the proto-object ($\tau \ll 1$, $V_p/c < 10^{-3}$), K - gain coefficient due to luminescence effect, $K=1-1000$ ($K=1$ for simple scattering). For the linear stage of perturbation evolution V_p could be estimated as (Zel'dovich, Novikov, 1975):

$$V_p = V_{p0}/(z + 1)^{1/2} \quad (2)$$

where $V_{p0}=600$ km/s at large scales of CMB anisotropy (CMBA) and factor 2-5 higher at small CMBA scales.

Luminescence effect is tempting for SSF search with limited sensitivity but high K may be expected in narrow z intervals (Dubrovich, 1997) while the simple mechanism of SSF formation operates in the wide field of z .

The optical depth τ of the proto-object may be calculated as (Dubrovich, Lipovka, 1995):

$$\tau = 8\pi^{5/2} d^2 (1+z)^{3/2} n_H \alpha \cdot [1 - \exp^{-h\nu/kT}] / 3hH_0, \quad (3)$$

$$h\nu/kT = hc/[kT_0\lambda_0(1+z)] \quad (4)$$

H_0 - Hubble constant, h -Planck constant, k -Bolcman constant, λ_0 - the rest wavelength, T_0 - CMBR temperature, $n_H = n_{0H} \cdot \beta$, where n_H - density of H , n_{0H} - critical density of atomic hydrogen $HI(10^{-5})$, β - a real density of H in proto-object which may be less or much more than unity ($\beta \geq 4 \cdot 10^{-2}$), d - dipole moment, α - abundance, $\alpha = 10^{-8} - 10^{-17}$ for different molecules and conditions in Early Universe.

Let us consider LiH , H_2D^+ , HeH^+ HD^+ primordial molecules.

LiH is a very important molecule, because it consists of primordial Li. Its abundance is a good test for the epoch of nuclear synthesis in the Early Universe. Its large dipole moment and relatively low frequency of the rotational and rovibrational transitions lead to a high value of K . But, unfortunately, some difficulties with the chemical processes of forming this molecule lead to a not too optimistic prediction for its abundance $\alpha = 10^{-11} - 10^{-17}$. The rest

wavelengths of LiH are $\lambda_r=676 \mu\text{m}$ (rotational transition), $\lambda_v=7.1 \mu\text{m}$ (rovibrational transition).

HD⁺ is also an important molecule due to the presence of primordial deuterium D. The abundance of D is about 5 orders of magnitude larger than that of Li. But HD⁺ has a dipole moment about 10 times less than LiH and a cross-section which is 100 times smaller. Another small factor is the abundance of H⁺ at redshift $z = 200$, which might be about relative to that of neutral hydrogen. Due to the relatively high frequency of the rotational and rovibration transitions, the resulting value of K is not very large. Yet, if high sensitivity were reached, this molecule might be seen. The rest wavelengths of HD⁺ are $\lambda_r=227 \mu\text{m}$, $\lambda_v=3.0 \mu\text{m}$.

HeH⁺ does not have any low abundance species. There are only two small factors which lead to a low abundance: a high rate coefficient for destruction (by electron recombination and collisions with the neutral atoms of hydrogen) compared with the very small rate coefficient of formation, and small abundance of H⁺ at high redshift. It might be the most likely molecule to be searched for due to more optimistic predicted abundance $\alpha = 10^{-8} - 10^{-15}$. The rest wavelengths of HeH⁺ are $\lambda_r=149 \mu\text{m}$, $\lambda_v=3.3 \mu\text{m}$.

H₂ D⁺ is the simplest triatomic molecule with a high dipole moment. It contains primordial deuterium D. Due to the presence of very low frequency transitions in its spectrum the value of K can be very high. It is very important that the redshift of the H₂ D⁺ recombination is relatively high. The rest wavelengths of H₂ D⁺ are $\lambda_r=1920 \mu\text{m}$, $\lambda_v=4.5 \mu\text{m}$.

The expected abundances of these molecules in the Early Universe are discussed by many authors (Lepp and Shull,1984, Puy et al, 1993, Palla et al, 1995, Maoli et al, 1996, Stancil et al, 1996).

One of the main observational effects caused by expansion of the Universe is the redshift of photons, expressed as $\lambda_{obs} = (z + 1) \lambda_{em}$, where λ_{em} is the emitted or rest wavelength of the photon. So, if an object contains a gas of any molecules and has a z redshift, it can only be seen at different but discrete frequencies $\nu_i = \nu_{oi}/(1 + z)$, where ν_{oi} is a discrete set of the molecule's rest transition frequencies. And vice versa, if some object is seen at given frequency ν_i this object can have the redshifts $z_i = \nu_{oi}/\nu_i - 1$.

The final spectrum depends on the angular size of the object θ . The angular size θ and the frequency bandwidth $\Delta\nu/\nu$ depend on linear size L (for a spherical shape object) and z of the object to be observed. For small z the angular size of the object(if the linear size is constant and equal to L) is decreasing with moving away, but it grows for z larger than some value. Exact relations between θ and z in this model contain the Ω_m and Ω_Λ parameters, which are the ratios of the matter n_m and "vacuum" densities to the critical

density n_c respectively ($\Omega_m + \Omega_\Lambda = 1$). The fact that the cloud occupies the interval of redshifts z means that if it radiates or reflects the radiation locally in sufficiently narrow lines, all the radiation occupies the frequency interval $\Delta\nu$, moreover $\Delta\nu/\nu = \Delta z/(1+z)$. Scattering by molecules in several lines leads to superposition of images of different proto-objects at different z . Taking into account Δz dependence on L and Ω (Sahni, Starobinsky, 2000) we have:

$$\Delta\nu/\nu \approx \theta\phi(z)[\Omega_m(1+z)^3 + \Omega_\Lambda]^{1/2}(1+z)^{-1}, \quad (5)$$

$$\phi(z) = \int_0^z 1/\sqrt{\Omega_m(1+z)^3 + \Omega_\Lambda} dz, \quad (6)$$

$$\theta = (H_0 L/c)(1+z)/\phi(z), \quad (7)$$

$$\Delta\nu/\nu \approx (H_0 L/c)\sqrt{\Omega_m(1+z)^3 + \Omega_\Lambda}. \quad (8)$$

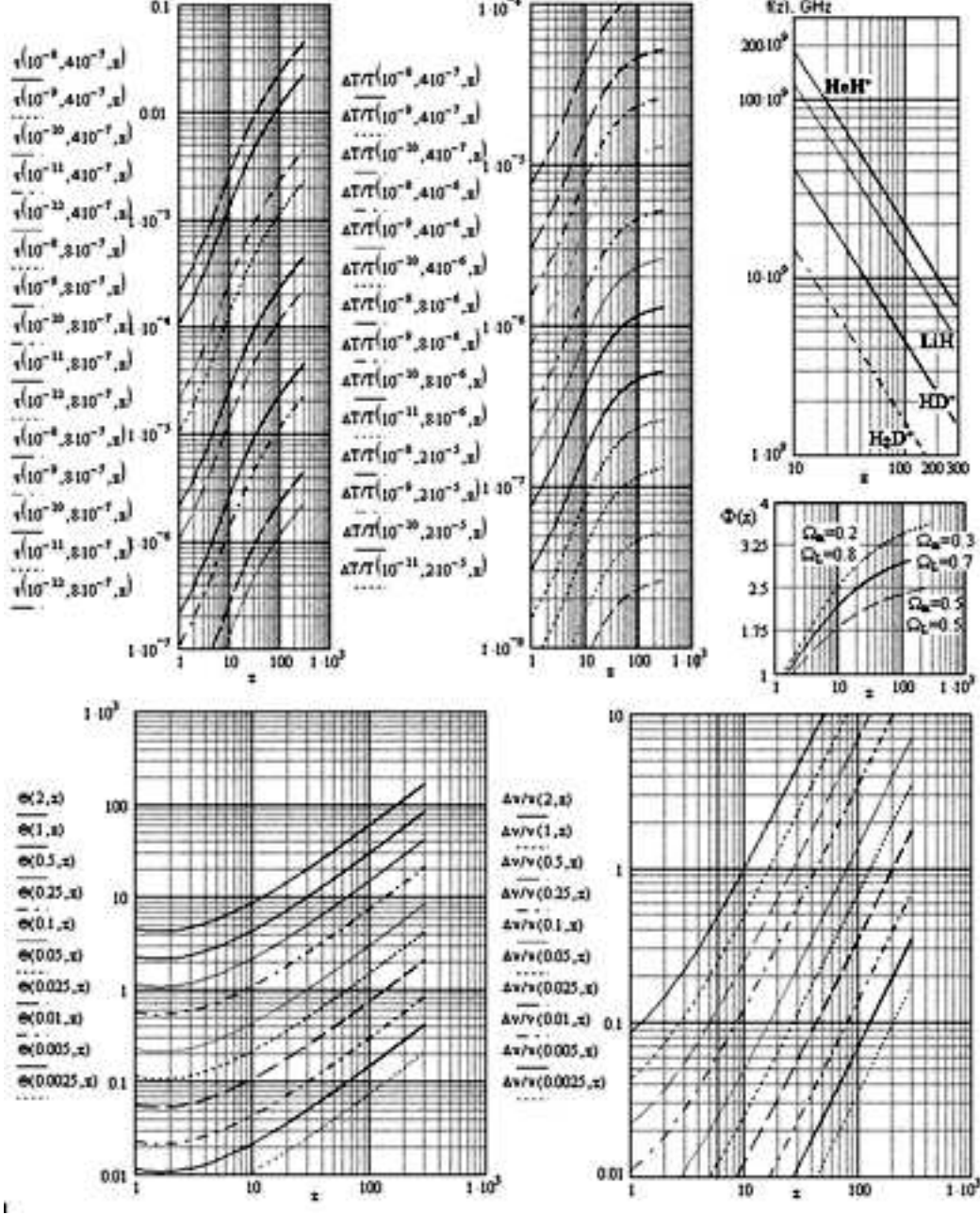
If we simultaneously observe CMBR in two receiver channels with frequency difference $\Delta\nu$, the SSF with an angular size larger than some critical θ_c are seen at both receiver channels. If the size of the fluctuations is smaller, they are only seen in one of the receiver channels, another one will detect background noise only (Dubrovich, 1982). In this case the correlation function of these two observations will be within noise to zero at small scales and different from zero at angular scales greater than θ_c . Then the difference signal of the two channels is not zero at the scales less than $\theta_c(L_c)$. Frequency separation $\Delta\nu/\nu$ of receiver channels determines a critical scale of proto-objects L_c and scales $L < L_c$ remain in difference of two channels. Frequency resolution or the channel bandwidth $\Delta\nu/\nu$ determines the optimal scale L_{opt} which has the best S/N at given z . The channel bandwidth should be a few times less than frequency separation and $L_{opt} < L_c$.

The above consideration is correct for objects freely expanding over the Universe in accordance with the Hubble law. But at the sufficiently late stages the deceleration of their expansion takes place and contraction begins due to self-gravitation. In this case the width of the line can be considerably smaller, and the amplitude larger (Zel'dovich, 1978).

Fig.1. shows expected $\tau(\alpha, n_H, z)$, $\Delta T/T(\alpha, n_H, z)$, $\phi(\Omega_m, \Omega_L, z)$, $\theta(L, z)$, $\Delta\nu/\nu(L, z)$ for HeH^+ ($\lambda_0 = 1.49 \cdot 10^{-2}$ cm, $d = 1.66$ deb) and $K=1$. According to Fig.1 an optimistic level of $\Delta T/T = 2 \times 10^{-5} - 2 \times 10^{-6}$ may be achieved with $\alpha = 10^{-9} - 10^{-10}$. Expected observational frequencies $f(z)$ are given in Fig.1. for rotational transitions ($I=0$) of LiH , H_2D^+ , HeH^+ HD^+ . For $\phi(\Omega_m, \Omega_L, z)$ calculation we used Ω_m and Ω_L which are discussed in several Cosmological models and recent CMBR experiments (Ruhl et al, 2004, Miller, 2004).

Let us limit possible physical proto-object scales L in the Early Universe: 2

Fig. 1. $\phi(\Omega_m, \Omega_L, z)$, $\tau(\alpha, n_H, z)\theta(L, z)$, $\Delta\nu/\nu(L, z)$, $\Delta T/T$, $f(z)$ for HeH^+



Mpc $> L > 0.002$ Mpc. The most of Cosmological molecules considered may exist at $z < 200$ and some at $z < 300$. Then possible angular scales θ for different $\Delta\nu/\nu$, L and z are calculated with (7),(8) and presented in Table 2. Table 2 shows that modern angular scales $\theta = 5' - 10'$ are still reasonable to search for large scale SSF at $z=20-30$ with $\Delta\nu/\nu=1-2\%$. Possible observational frequencies $f(z)$ for HeH^+ ($I=0$) are given in Table 3. Most of primordial molecules can radiate at several rotational transitions I that leads to SSF formation at set of frequencies $f_i(z)$. LiH has radiating transitions at $I=0,1,2,3,4,5,6,7$. The optical depth τ in molecular lines depends on I and in the case of thermodynamic

Table 2

Angular and spatial scales for HeH⁺(I=0)

$\Delta\nu/\nu, \%$	z_{min}	z_{max}	L_{max}, Mpc	L_{min}, Mpc	$\theta_{max} (')$	$\theta_{min} (')$
0.1	5	200	0.5	0.0025	1.4	0.14
0.5	10	200	1	0.015	4.3	0.85
1	10	200	2	0.025	8.6	1.4
2	15	200	2	0.05	11.5	0.3
4	25	200	2	0.1	17.3	5.7
5	30	200	2	0.15	20.1	8.5
6	35	200	2	0.17	22.9	9.6
7	40	200	2	0.2	25.8	11.3
10	50	200	2	0.25	31.4	14.2

Table 3

Observational frequencies f(z) in GHz for HeH⁺(I=0)

z	5	10	15	19	20	22	52	60	65
f	335.57	183.30	125.84	100.67	95.88	87.54	37.99	33.00	30.51

Table 4

Possible observational frequencies f(z) in GHz for LiH(I=6)

z	10	15	20	30	32	34	35	80	101
f	287.08	197.37	150.38	101.87	98.68	90.23	87.71	38.9	30.96

equilibrium for optically thin layer is (Dubrovich,1982):

$$\tau_{I,I+1} = \tau_0 \cdot (I + 1) \cdot \exp(-T_0 I(I + 1)/T) \quad (9)$$

where optical depth $\tau_0 = \tau(I=0)$ is given by (3), T_0 - temperature correspondent to energy of transition I=0-1, T- temperature of radiation at given z. For LiH extremum of τ lies at I=6 ($\lambda_0 = 0.95 \cdot 10^{-2}$ cm) and $\tau(I = 6)/\tau_0 = 2-4$. Possible observational frequencies $f_i(z)$ for LiH(I=6) are given in Table 4. Expected $\Delta T/T$ level for SSF caused by LiH with existing estimates of LiH abundance is less than 10^{-5} that can not be achieved in this experiment but we can set an upper limit of $\Delta T/T$ for LiH at z=30 as well.

If we realize a channel bandwidth of $\Delta\nu/\nu = 2\%$ in 3 mm band preferable or optimal linear scales for SSF search are $L = 1.5$ Mpc for HeH⁺(I=0) at z=20 and $L = 0.75$ Mpc for LiH(I=6) at z=30, correspondent angular sizes according to (7) are $10.7'$ and $7.5'$.

Recent WMAP polarization measurements have shown strong probability of

Table 5

Spatial scales L of peaks in CMBR power spectrum for different z

z	L_1, Mpc	L_2, Mpc	L_3, Mpc	L_4, Mpc
1000	0.22	0.11	0.073	0.043
100	1.99	0.99	0.66	0.39
50	3.72	1.86	1.24	0.74
30	5.79	2.91	1.93	1.16
20	8.08	4.04	2.69	1.62

an early reionization scenario with $z_r = 20(+10/ - 9)$ (Kogut et al, 2003, Page et al, 2006) due to Pop III stars (Wyithe, Loeb,2003) in Galaxy halos. SSF detection at $z=20-30$ may provide us with important information about ionization history of the Universe.

The question is which maximum proto-object scales are reasonable, could exist at $z=20-30$ or are connected with some known scales in the Universe. Let us compare them with spatial scales of primary CMBA. The angular scale of the first peak in primary CMBR power spectrum $\theta_1 \approx 50'$, the following CMBA peaks are $\approx 1/2\theta_1, 1/3\theta_1$, and $1/5\theta_1$ (see Fig.2 down). Then possible spatial scales L of 1-4 peaks in CMBR power spectrum for different z are given in the Table 5 with (7) and (6).

The above consideration shows that at $\Delta T/T=2 \cdot 10^{-5}$ level and with $\Delta\nu/\nu=2\%$ we can search for SSF which are the result of large scale proto-object motion with peculiar velocity relative to CMBR at $z=20-30$. These possible proto-objects are still less than spatial scale of the fourth peak in CMBR power spectrum (Table 5) which might be related to a proto-galaxy scale. With less $\Delta\nu/\nu$, higher sensitivity and multipole resolution we can approach to smaller spatial scales of proto-objects up to proto-star scales.

SSF firstly proposed as a new phenomena in (Dubrovich, 1977) is one of most promising secondary CMBA. SSF is non-isotropic spectral distortions of CMBR which are to be present at $z=300-10$. Homogeneous and isotropic spectral distortions of CMBR may be present at $z=6000-1000$ due to primordial Helium and Hydrogen recombination (Dubrovich, 1975, Dubrovich, Stolyarov, 1995, Dubrovich, Shahvorostova, 2004, Dubrovich, Grachev, 2004). Non-isotropic distortions of CMBR similar to SSF may be present in this epoch at lower $\Delta T/T$ level as well (Dubrovich, 1977/2). Calculation of this effect in more details at $z=1000-1100$ is done in (Rubino-Martin, Mernandez-Montegudo and Sunyaev, 2005).

3 Simulation of SSF

Let us remind that CMBR temperature fluctuations are expanded in spherical harmonics (Peebles, 1993, Peacock, 1999):

$$\Delta T(\theta, \phi)/T_0 = \sum_{l=0}^{\infty} \sum_{m=-1}^l a_{lm} Y_{lm}(\theta, \phi), \quad (10)$$

The angular power spectrum C_l of $\Delta T/T$ can be related to the autocorrelation function $C(\theta)$ as:

$$C(\theta) = 1/4\pi \sum_l (2l+1) C_l P_l(\cos\theta), \quad (11)$$

where P_l are Legendre polynomials, l -multipole moment and $C_l = \langle |a_{lm}|^2 \rangle$. Theoretical predictions of ΔT are usually quoted as

$$(\Delta T_l)^2 = l(l+1) C_l / 2\pi, \quad (12)$$

$$\Delta T_l = \sqrt{l(l+1) C_l / 2\pi}, \quad (13)$$

As we consider small-angle patches of the sky CMBR fluctuations $\Delta T = T - \langle T \rangle$ may be generated by evaluating the simple Fourier series (Bond et al, 1987):

$$\Delta T(\theta_x, \theta_y)/T = \sum_{n_u=0}^{N_u-1} \sum_{n_v=0}^{N_v-1} D(n_u, n_v) \exp[i \frac{2\pi}{L} (n_u \theta_x + n_v \theta_y)] \quad (14)$$

where L denotes the size of the simulated region in radians; (θ_x, θ_y) are Cartesian coordinates on the sky (spatial domain); (n_u, n_v) are coordinates of Fourier components D in spatial frequency domain, $\langle |D(n_u, n_v)|^2 \rangle = C_l$, $l = 2\pi/L \cdot \sqrt{n_u^2 + n_v^2}$.

For the search of SSF CMBR maps obtained in several spectral channels are to be studied and then processed by the special frequency-differential or the difference method (Dubrovich, Bajkova, 2004). The Difference method can be considered as an alternative method to the correlation function analysis. In this case we are interested in the first derivative of spatial distortions with respect to the frequency. The method used is based on the analysis of a difference of two CMBR temperature maps observed at different frequencies and reduced to one beam shape. Mainly, such a difference map contains information only

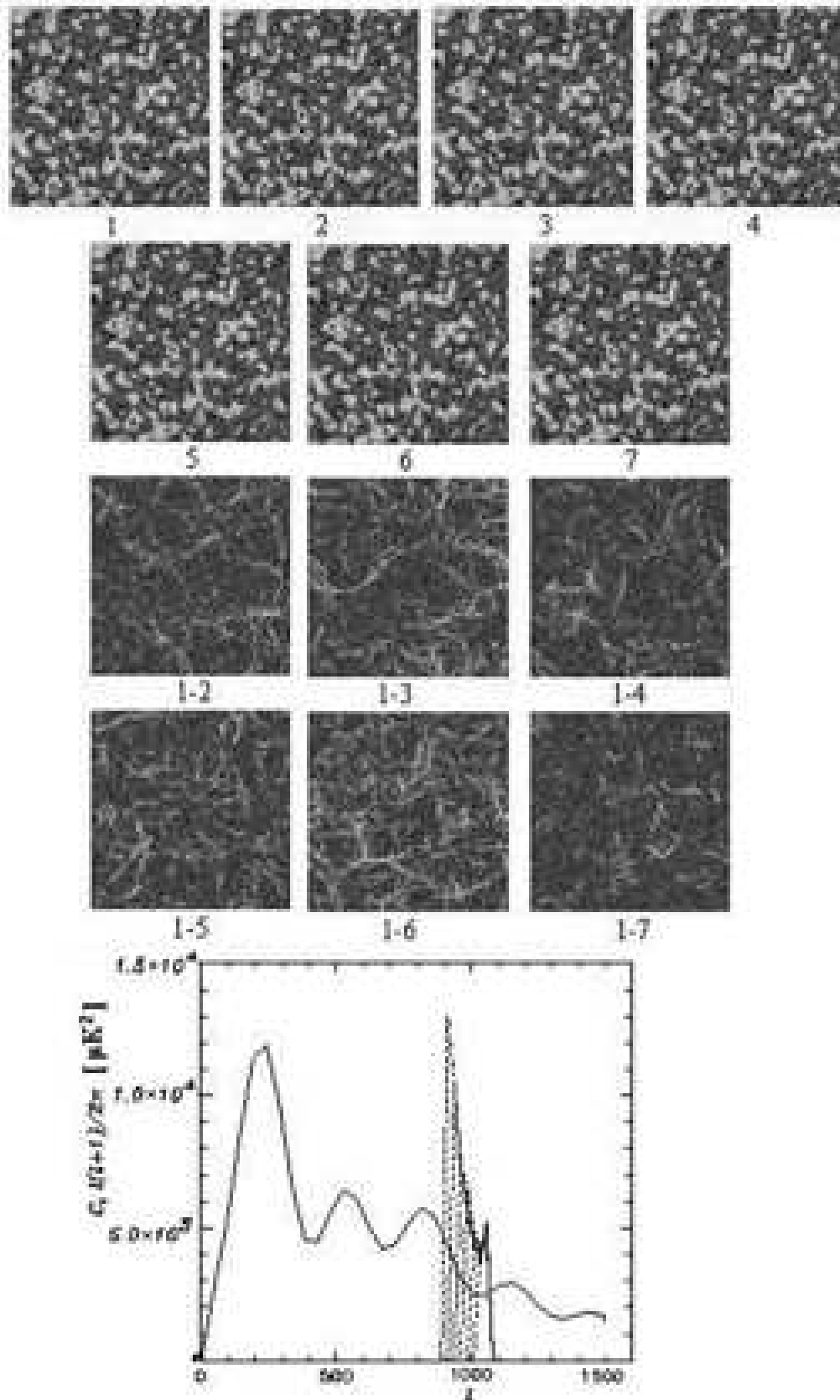
on the secondary fluctuations because the primary CMBR fluctuations present in both maps will be eliminated due to their black-body spectrum nature.

The procedure of SSF simulation is the following. Firstly CMB map is generated with a standard CMB power spectrum. Then amplitudes of FFT spectrum of CMB map are kept while phases are modified as random values uniformly distributed in the interval $0-2\pi$. A backward FFT gives us an approximation of CMB map which contains primary and secondary fluctuations in conditions of unknown theoretical power spectrum of SSF. The actual theoretical power spectrum of SSF is to be a subject of nearest energetic efforts, it is strongly needed for following SSF investigation.

Let the difference of the CMBR observation frequencies be equal to $\Delta\nu_1$. Let the limiting angular fluctuation size θ_1 corresponds to this frequency difference in accordance with equation (5). Obviously, the fluctuations of size larger than θ_1 will be seen at both maps. After subtraction of one map from the other the fluctuations of size larger than θ_1 will be mutually suppressed and the remainder map will contain only the fluctuations smaller than θ_1 . Evidently, this fact can be seen also from angular power spectrum of this map which is close to zero at frequencies with multipoles $l < l_1$ and different from zero at $l > l_1$, where $l_1 \approx 1/\theta_1$ is the break of the spectrum. Now let the difference of two frequencies be $\Delta\nu_2$, where $\Delta\nu_2 > \Delta\nu_1$. The angular size θ_2 corresponds to this frequency interval. Obviously, $\theta_2 > \theta_1$ in accordance with equation (5). In this case we will see at the difference map the fluctuations with size smaller than θ_2 and the corresponding angular power spectrum will have the break at $l_2 \approx 1/\theta_2 < l_1$.

Our CMBA model also includes convolution of expected CMBA maps with a simulated radio telescope beam and adding a pixel noise. Differential maps are preliminary processed to decrease the noise in given power spectrum region. Let convolved CMBR maps have spatial scales $l_{min} \div (l_{max}-m\Delta l_m)$, then the spatial scale of differential maps is $(l_{max}-n\Delta l_m) \div l_{max}$, where $m=0,1,2,\dots$, $\Delta l_m/l$ corresponds to $\Delta\lambda_m/\lambda$ (2% in our case). Let us limit l_{max} in the simulation by $l=1056$ which is near to the lowest reasonable limit of l_{max} in the ground based MM-wave SSF experiment. We will use in simulation a standard Λ CDM CMBR model (Spergel et al., 2003, Spergel et al, 2006) with parameters: $\Omega_b \times h^2=0.2(H_0/100 \text{ km/sMpc})$, $H_0 = 65 \text{ km/sMpc}$, $\Omega_\lambda=0.65$, $\Omega_M = 0.3$, $n=1$, $h=0.65$. Initial single frequency CMBR maps (Fig.2 up) $15^\circ \times 15^\circ$ (128x128 pixels) have $l=3-1056(1)$, $l=3-1032(2)$, $l=3-1008(3)$, $l=3-984(4)$, $l=3-960(5)$, $l=3-936(6)$, $l=3-912(7)$, all $\sigma(\text{quadratic sum})=25902$. Difference maps (Fig.2 down) have $l=1032-1056(1-2)$, $\sigma=14.4$, $l=1008-1056(1-3)$, $\sigma=21.3$, $l=984-1056(1-4)$, $\sigma=32.4$, $l=960-1056(1-5)$, $\sigma=42.9$, $l=936-1056(1-6)$, $\sigma=60.8$, $l=912-1056$, $\sigma=87.6$ with the angular power spectrum corresponding to Λ CDM model for initial (solid line) and differential (dashed line) CMBR maps (Fig.2 middle).

Fig. 2. Initial single frequency CMBR maps $15^\circ \times 15^\circ$ (128x128 pixels) (up), difference maps (middle), power spectrum of ΔT corresponding to Λ CDM model for initial (solid line) and differential (dashed line) CMBR maps (down)



It was shown in (Dubrovich, Bajkova,2004) that the Difference method may be used when S/N ratio for each map is 1.44. In case of higher level of noise a more complicated preliminary signal processing directed to decreasing the noise in the given CMBR spectrum region would be required. Fig.3 demonstrates predicted difference SSF map without an instrumental noise(up) and with white instrumental noise (down) added in single frequency maps with S/N=1.17. Power equalization method of Wiener filtration (Gorski, 1997) was applied in this case as signal preliminary processing to decrease the noise in given power spectrum region. In spite of a correlation coefficient of two difference maps of Fig.3 is less than 0.15 the power spectra of the difference signal after Wiener filtration are similar (Fig.3 right) that is the most important to recognize SSF in a real SSF search experiment. But this is true for white instrumental noise and we concentrate our efforts in section 4 to avoid or minimize abnormal instrumental pixel noise in the SSF search experiment.

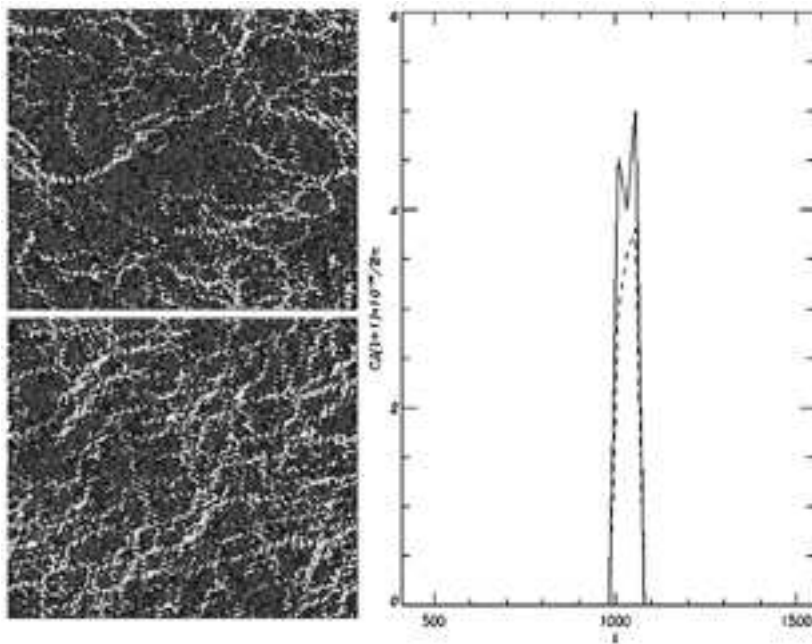
It was assumed in above simulation that the observed CMBR maps consist only of the primary and secondary CMBR fluctuations with some additive white instrumental noise. However, in practice the CMBR detected maps in addition contain a number of astrophysical foregrounds such as extragalactic unresolved sources, free-free and synchrotron radiation, SZ effect, Galactic dust and so on. Astrophysical foregrounds are characterized by considerably low value of spectral index as compared with the analyzed secondary CMBR fluctuations and are successfully eliminated in difference maps.

4 A concept and strategy of SSF Experiment

Up to now practically all CMBR ground based and space experiments study primary CMBA which has black body spectrum. Primary CMBA was 30 years under investigation at RATAN-600 radio telescope since 1977 (Parijskij, Korkov, 1986, Parijskij et al, 2005).

First attempts of SSF observations were done in 1992 at IRAM MM radio telescope with the upper $\Delta T/T$ limit $2 \cdot 10^{-3}$ at 1.3 mm (De Bernardis, Dubrovich et al, 1993) and in 2001 at RATAN-600 (the near pole survey) with the upper $\Delta T/T$ limit 10^{-3} at 6 cm (Gosachinskii, Dubrovich et al.,2001). Surplus frequency resolution of the existing spectrum-analyzers (30 MHz and 20 KHz) increased $\Delta T/T$ limit in both cases. The Far Infrared Absolute Spectrometer(FIRAS) instrument has shown that CMB has ideal black body spectrum from 60 GHz to 600 GHz and CMB temperature is 2.725 ± 0.001 K(Fixsen, Mather,2002). Then Fixsen et all reported about an effort to measure distortions of CMB black body spectrum due to of various processes in Early Universe. This attempt was done in ARCADE balloon-born experiment where CMB temperatures were measured at 10 GHz and 30 GHz with accuracy \pm

Fig. 3. Predicted difference SSF map without noise(left up) and with white noise (left down), S/N=1.17, the correspondent power spectrum without noise - solid line and with white instrumental noise - dashed line (right)



0.010 K and ± 0.032 K (Fixsen et al, 2004). In this paper we suggest a concept and strategy of the SSF experiment with $\Delta T/T$ limit $2 \cdot 10^{-5}$. High absolute measurement accuracy is not necessary in this experiment as we need to measure differential temperatures in nearby receiver channels without measuring absolute CMB temperatures.

Fig. 4. Multibeam Solar Radio Telescope (MSRT) of Tuorla Observatory, Finland



Simulation of possible SSF experiment is done for MSRT (Khaikin et al, 2002,2003), Tuorla Observatory, Finland (Fig.4) equipped with a 7x4 beam cryo-microbolometer array at 3 mm with RF multiplexer providing up to 7 spectral channels in each beam. The scheme of the experiment is given in Fig.5. Firstly idea of such an experiment is suggested in (Dubrovich, Bajkova, Khaikin, 2004, Khaikin, Dubrovich, 2004, Khaikin, Luukanen, Dubrovich, 2005). In this paper we develop the concept and present simulation results of a possible experiment.

RF filters

The challenge is to split RF band in front of bolometers. If superconducting Nb microstrip resonant $\lambda/4$ stub filters are used in RF multiplexer (RFM) the in-band transmission can approach unity due to negligible loss of the superconductor. To simplify a multiplexer design the number of filters and spectral channels may be reduced to 5 or even 3. A wideband microstrip superconducting frequency multiplexer is applied in front of TES bolometers in SAMBA(Superconducting Antenna-coupled Multifrequency Bolometric Array), where low loss and excellent out-of-band rejection is demonstrated at 3 frequencies of MM band (Goldin et al, 2003). Antenna-coupled TES bolometer with an integrated microstrip BP filter at 217 GHz is applied for a bolometer array in a ground based CMB polarization experiment (Myers et al, 2005).

Another way to split radio frequency band in a bolometric receiver is to build a quasi-optical filter based on metal mesh filters(MMF) or frequency-selective surfaces (FSS). A review of quasi-optical MMFs is given in (Ade et al, 2006). A few possible designs of cryogenic MMFs with bandwidth up to 6% at 1-3 mm are given in (Page,1994). 3 cryogenic filter wheels with several bandpass filters, are under development now in Columbia University for Millimeter Bolometric Array Camera (MBAC) to provide 5-10% frequency resolution in one octave MM band from 150 GHz to 300 GHz at Atacama Cosmology Telescope(ACT).

FSS may be also used to separate in space radio telescope foci in which several feeds or arrays at different frequencies may be placed (Kasyanov, Khaikin, 2004). But it is difficult to achieve frequency resolution with MMF or FSS better than 5% and superconducting N_b microstrip resonant filters are more effective in our case.

Array feeds

We consider several variants of an array feed. As a narrow flare corrugated horn is difficult to build in 3 mm band a trimode conical horn may be used to provide a small flare angle with an acceptable sidelobe level (less than -20 dB in E/H plane) and low frequency cut-off near 87 GHz. A smooth-walled spline-profile horn(Granet et al, 2004) is an alternative to both corrugated and trimode horns and it allows us to achieve an identical radiation pattern in E/H plane in the band, low sidelobe level(less than -25 dB), more tight array packaging and lower manufacture cost. We are in final stage now to build and test such a horn for array applications at lower frequencies (30 GHz-38 GHz) in cooperation with C.Granet(CSIRO)(Khaikin et al,2007).

Multipole resolution

A 2 m precise carbon fiber MSRT dish (Khaikin et al,2002) allows us to work in 100 GHz and 150 GHz bands but the second one is much more difficult due to higher atmospheric attenuation and antenna scattering background. Angular resolution of MSRT is 7'-6' at 88 GHz-100 GHz that is enough for a large scale SSF experiment and corresponds to $l_{max}=\pi/\theta=1542-1800$ (for full sky coverage) the same as at Planck (7', $l=1542$) and twice better than at WMAP($l_{max}=750$). Nevertheless for a ground based or balloon experiment $\Delta l < l < l_{max} - \Delta l$, where $\Delta l = 2\pi/M$ (size of the symmetrical map) and actual spatial resolution of MSRT is not higher than $l=1200-1500$ for partial sky coverage. In Boomerang balloon experiment actual resolution was less than $l=1025$ at 150 GHz(de Benardis et al.,2002). $1000 \geq l \leq 1500$ seems to be optimal for SSF search at current stage. At higher l with the low frequency resolution S/N ratio falls. Besides, in ground based experiments with higher angular resolution such as Cosmic Microwave Imager (CBI) (Readhead et al,2004) with $l_{max}= 3500$ point sources were a serious problem at 26-36 GHz

as the power spectrum of primary CMBA falls rapidly with l while the point source contribution grows as l^2 in the band. Point source contamination is still dangerous at 3 mm at higher l if secondary CMBA has a falling spectrum. Some secondary CMBA may have inverted C_l spectra when the magnitude of C_l grows at higher l (Doroshkevich, Dubrovich, 2001). However SSF search at $l > 1500$ needs both higher sensitivity and higher frequency resolution which contradicts each other.

Chopping mode

A multifeed or receiver array is needed in a SSF experiment to get a CMBR map in an unmovable radio telescope mode (preferable) or to accelerate mapping in a scanning mode (less preferable because of variable instrumental effects). We plan to use a chopping mode to reduce an abnormal instrumental noise and atmospheric effects. A chopper with beam deviation θ_{ch} will distort power spectrum of SSF due to filtration of scales $\theta > \theta_{ch}$ and changing the amplitudes at scales $\theta < \theta_{ch}$ but this is not so dangerous in the task of SSF search. The main role of the chopper is to suppress uncorrelated residual 1/f noise of different bolometers which can not be eliminated in difference maps.

Calibration

Identical and stable calibration of all receiver channels is very important in this experiment. It may be produced quasi-optically by a lens, forming a lateral plane wave for a whole array. A high stable noise generator with a direct coupler or a matched black body load is placed in the lens focus. A calibration source must be put in a reverse two level thermostat realizing 0.1 K accuracy at the first and not less than 0.01 K accuracy at the second level.

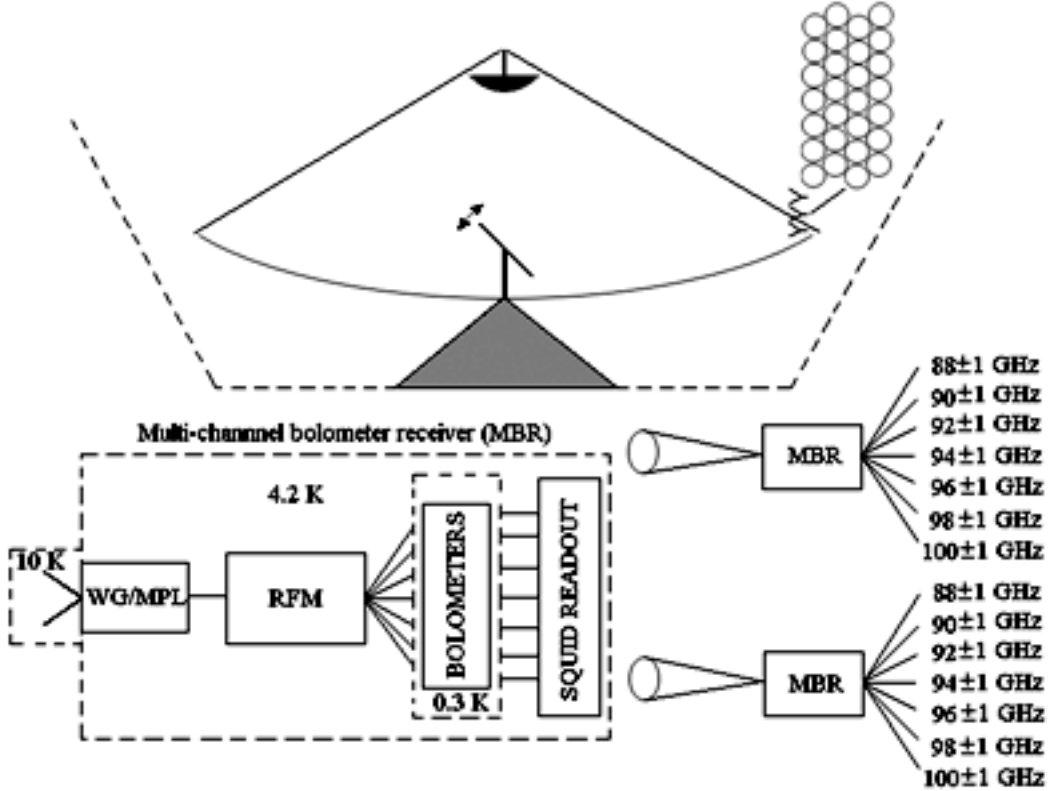
CMBR map

According to our concept MSRT central beam is fixed near the North Celestial Pole (NCP) at $\delta = 86^\circ$ to increase cosmic source passing time via the beam up to 348s -402s and to observe the $1^\circ \times 8^\circ$ strip preferably in low culmination from $\alpha = 8^h 00^m$ to $16^h 00^m$ at high Galactic latitudes. Actual spatial resolution of a combined CMBR map in the scheme of Fig.5 is $6'-7'$ (HPBW). The long-length focus Cassegrain scheme with $m = (e+1)/(e-1) = 10-11$ (eccentricity $e > 1$) gives us negligible aberrations of off-axis beams but requires more complicated array feeds. A short-length focus Cassegrain radio telescope scheme gives us unacceptable level of off-axis aberrations(Khaikin, Luukanen, 2003).

Antenna characteristics

We simulated some antenna characteristics for the scheme of the experiment given at Fig.5. Antenna parameters are $D = 2$ m, $d = 0.3$ m, $F/D = 0.435$, interfocal distance $f = 150$ cm, feed flare angle is 12 deg. Simulated characteristics are

Fig. 5. Suggested scheme of the experiment (up), multichannel bolometer receiver (MBR) scheme with RF multiplexer (down)



given in Table 6. Multibeam Focal Plane Array (FPA) configuration presented in Fig.5 allows us to avoid undersampling in a survey mode. For simulation of the multibeam radiation pattern, calculation of some other antenna characteristics (illumination, aperture, spillover, sidelobe efficiencies, beam overlapping level etc.) Focal Plane Array Simulation (FOPAS) program package has been used (Khaikin, 2005). FOPAS takes into account geometry of a single or dual reflector radio telescope, expected aperture distribution or the beam pattern of an ideal broadband feed, the feed removal from the focus and off-axis aberrations. FOPAS allows us to optimize FPA geometry with the beam spacing and the overlapping level which are optimal for the given astrophysical task. The task of multibeam FPA optimization is also considered in (Majorova, Khaikin, 2005). Multibeam radiation pattern simulated with FOPAS is given in Fig.6.

TES bolometers

We consider Transition Edge Sensors (TES) as cryo-bolometers for this experiment (Khaikin, Luukanen, Dubrovich, 2005). The lateral dimension of TES is less than 10 microns (microbolometer) and standard lithographic techniques may be used to build arrays of 100-1000 sensitive elements.

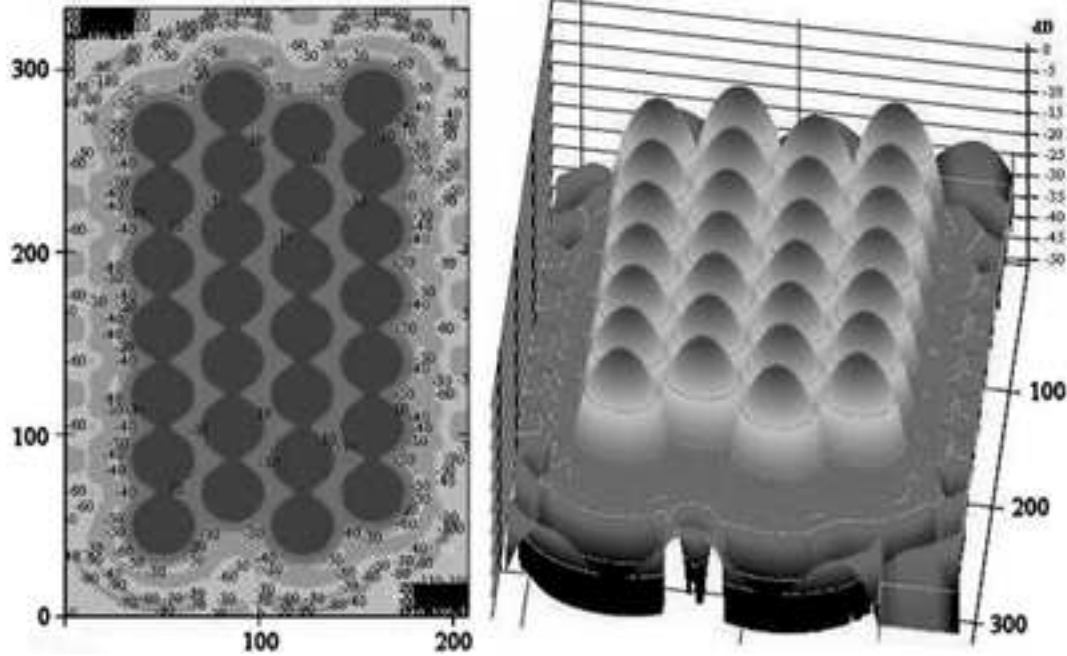
Photon and phonon Noise Equivalent Power (NEP) and Noise Equivalent

Table 6

Simulated antenna characteristics

Number of beams	Feed taper, dB	HPBW at 88-100 GHz, arcmin	FSL, Db	Beam overlapping level, dB
28	-10/-13	7-6	21/24	-0.45
Spillover efficiency, dB	Blockage efficiency dB	Illumination efficiency	Ruze efficiency (94 GHz)	Antenna efficiency (94 GHz)
-0.45	-0.23	0.91	0.75	0.51

Fig. 6. Simulated multibeam radiation pattern of MSRT at 100 GHz, the feed taper is -13 dB



Temperature Difference (NETD) of TES for the ground based SSF experiment are considered in (Khaikin, Luukanen, Dubrovich, 2005). An expected phonon NEP of a cryo-microbolometer with the physical temperature of 0.3 K is $<1 \cdot 10^{-17} \text{ W/Hz}^{1/2}$. We do need the physical temperature near 0.3 K (Fig.5) as NEP of TES dramatically grows at higher physical temperatures (Luukanen, Pekola, 2003). Photon NEP from radio telescope antenna and atmosphere is not less than $2 \cdot 10^{-17}$ in good atmospheric conditions. This will give us $\sigma=1.0-2.0 \text{ mK s}^{1/2}$ sensitivity per beam per channel (2 GHz bandwidth) in the best atmospheric conditions with $T_{atm} < 20 \text{ K}$ (the lowest atmospheric opacity). In 8x8 element planar bolometer array at 90 GHz for GBT operating temperature is 450 mK, which limits NEP of TES bolometers to

2×10^{-17} W/Hz^{1/2} (Benford et.al,2004). The physical temperature T_p of an antenna coupled with a superconducting bolometer must be chosen to provide a photon NEP $< 10^{-17}$ W/Hz^{1/2}. For rather high radiative antenna efficiency $\eta=0.9$ and $T_p=300$ K an additional photon noise from an antenna is 10^{-16} Wt/Hz^{1/2} and cooling of antenna (horn) up to at least 10 K is necessary to provide its own photon NEP at less than 10^{-17} Wt/Hz^{1/2} level (Khaikin, Luukanen, Dubrovich,2004)(Fig.5). For deep cryogenic cooling Sorption He^3 coolers at 0.3 K of Applied Physics Institute of RAS in Nizhnij Novgorod may be used (Vdovin, 2005).

Some ground based CMBR projects (Lawrence et al,2004) chose an alternative way and are being built cryogenic MMIC MM-wave cameras with expected sensitivity of $500 \mu K s^{1/2}$ in continuum in 3 mm band. We have considered such alternative as well. InP MMIC LNA at 15 K with a broadband subharmonic mixer and IF microstrip 10 channel multiplexer may give us 4-5 mKs^{1/2} per beam per channel (1% bandwidth) at 85 GHz -105 GHz (Khaikin et al, 2004).

Sensitivity in the experiment

The actual reachable integration time of a bolometer depends on the Knee frequency f_{kn} in its noise power spectrum. In a bolometer case f_{kn} may be reduced from tens of Hz to tens of mHz by biasing the bolometer with an AC current and synchronous demodulation in readout electronics (Crill et al, 2002). $f_{kn}=10$ mHz was reached by AC biasing of bolometers in a 144 pixel cryo-bolometer array BOLOCAM at 140-270 GHz (Mauskopf et al., 2000). With AC biasing of the TES bolometers we expect $f_{kn}=20$ mHz. In the effective chopping mode with chopper frequency $f_{ch}=5$ Hz $f_{kn}=5$ mHz may be reached then 3-4 minutes integration time becomes available. Using a 100 ms sampling rate for $f_{ch}=5$ Hz and 170 s synchronous integration time we can reach σ of thermal noise not worse than 0.1-0.2 mK per beam per pixel. Four $1^\circ \times 8^\circ$ maps (128x7 pixels) are to be recorded during about 8 hours in clear cold winter nights (after Sunset and before Sunrise) and then combined into one map (64x14 pixels) with minimum angular resolution $6' \times 6'$ and a noise factor of $1/2^{1/2}$ in comparison with initial maps. 20-25 identical maps must be summed for 20-25 clear cold nights with low atmospheric opacity in order to reach $30 \mu K$ σ of thermal noise in the averaged single frequency maps. We expect contribution of non thermal instrumental noise, atmosphere and foregrounds in differential maps up to $30 \mu K$ as well. So we may expect total $\sigma = 50-55 \mu K$ in differential maps.

Atmospheric limitations

Big efforts have to be made to reduce the contribution of instrumental and foreground effects at $\Delta T/T=10^{-5}$ level that corresponds to 10^{-7} of ambient temperature. Some instrumental effects such as 1/f noise, ground spillover, ra-

diometric offset may be comparable with an atmospheric noise but their contribution may be significantly reduced in the ground based experiment. Atmospheric fluctuations are to be effectively suppressed with a chopper while high atmospheric attenuation is the most dangerous for a ground based MM-wave SSF experiment with cryo-bolometers. Atmosphere gives the main limitation in sensitivity in MM wave ground based SSF experiment with cryo-bolometers as it will contribute up to 80% in a system temperature and in some cases may saturate (overheat) a cryo-bolometer. The bolometer must be able to absorb up to 1 pW in order to avoid saturation with photon NEP $\geq 2 \times 10^{-17}$ Wt/Hz^{1/2}. This requires a rather high dynamic range D which is the ratio of the maximum power detected to the minimal detectable power. For expected sensitivity 1 mK s^{1/2} D must be not worse than 45 dB. In fact only days with lowest atmospheric opacity (lowest water vapour content) may be used for such an experiment at sea level. It was shown by a ‘‘tipping curve’’ method that typical atmospheric opacity at MSRT site in zenith τ_z is 0.2 dB at 36.5 GHz for dry clear Autumn nights (Khaikin et al, 2003) that gives predicted τ_z at 94 GHz 0.3 dB - 0.5 dB in clear cold winter nights with lowest integrated water vapour content ($< 2g/m^3$). An effective beam wobbling made it possible to reduce residual atmospheric noise ΔT_{atm} and spillover ΔT_{spill} up to 10 μ K at 40 GHz in SK CMBR experiment in Canada (Wollack et al, 1994), where the radiometric offset was less than 7 μ K per day for all observations. A special ground screen (height up to 3 m) is to be installed near MSRT (Fig.5) to avoid the contribution of the hot atmosphere and ground via sidelobes, spillover and scattering background and provide $T_{AO} = 33$ K at high elevation angles including own antenna temperature, atmosphere (20 K) and CMBR(Khaikin, Luukanen, Dubrovich,2005). The residual non-thermal instrumental noise must be significantly reduced up to 30 μ K in differential maps while thermal noise grows by a factor 2^{1/2}in comparison with single frequency maps. Non-thermal noise can not be reduced lower in difference maps due to residual abnormal (1/f) instrumental noise, some difference in radiation patterns, in amplitude-frequency characteristics of the channels and some difference in atmospheric effects within 12% bandwidth.

In spite of atmospheric limitations a ground based SSF MM wave experiment has advantages in the cost, flexibility and possible duration. In space conditions TES bolometers may give one - two orders better sensitivity. In (Ali et al, 2003) NETD=25 μ K/s^{1/2} per pixel is expected in space for CMBR at 90 GHz for 100 TES detectors with the physical temperature less than 0.1 K and NEP= 2×10^{-18} Wt/Hz^{1/2}. Yet, most of new generation MM wave CMBR projects chose multi-element bolometer arrays to reach highest sensitivity in the ground based experiment. $NET_{CMBR} = 260 - 280 \mu K s^{1/2}$ per detector must be reached in 1000 element array of TES bolometers at 10 m South Pole Telescope(SPT) in 20% bandwidth at 95 GHz and 150 GHz(Ruhl et al, 2004). Millimeter Bolometric Array Camera(MBAC) with 3 1000-element TES bolometer arrays at 150 GHz/220 GHz/270 GHz is under development now for

Table 7

Expected characteristics of the experiment

Alpha, hours	Delta, degrees	Multipol moment l	Frequency band, GHz	Frequency resolution, %
8-16	86	1200-1500	88-100	2
Sensitivity per beam, $\text{mKs}^{1/2}$	Integration time, s	Integral sensitivity of the experiment, micro K	dT/T	Duration of the experiment
1-2	170	50-55	2×10^{-5}	Winter season

6 m Atacama Cosmology Telescope(ACT) Project (Fowler, 2004). Expected MBAC sensitivity to CMBR is $300 \mu\text{K}/500\mu\text{K}/700\mu\text{Ks}^{1/2}$ per detector

Astrophysical Foregrounds

In a ground based experiment at sea level atmospheric effects contribute much more than astrophysical foregrounds nevertheless we should take them into account to better prepare the experiment. Galactic and extragalactic dust emission will significantly dominate at 3 mm over other foreground effects such as discrete and diffuse sources, galactic synchrotron and free-free emission, hot clusters of galaxies. Dust fluctuations are seen on all angular scales from $2'$ to tens of degrees on IRAS data (Low et al.,1984). Antenna temperature is $T_a \sim \nu^{\beta_d}$, where β_d is the spectral index which depends upon the emissivity of the dust and lies in the range of 1.5-2.2 according to COBE, IRAS and WMAP data. After 60 GHz Galactic and extragalactic dust dominate and we should carefully chose CMBR map coordinates in dust free areas of the Universe at high Galactic latitudes. The full sky thermal dust map based on data from IRAS and COBE using MEM procedure shows a wide range of temperatures from $400 \mu\text{K}$ to $15 \mu\text{K}$ in W band of WMAP (94 GHz) (Bennet et al, 2004). Contribution of dust emission is to be significantly eliminated in differential maps as this component must be well enough correlated in single frequency maps due to its black-body spectrum.

5 Final remarks

As it was shown in section 2 the expected signal ($\Delta T/T$ of SSF) depends on many Cosmological parameters and conditions in Early Universe such as $\Omega_m, \Omega_\Lambda, \Omega_b, n_{0H}, \alpha, V_p$ and others while the best S/N ratio at given z also depends on $\Delta\nu/\nu$. It is extremely difficult to predict the most probable combina-

tion of these parameters at different z in Early Universe and SSF experiments are urgently needed to set SSF an upper limit at $\Delta T/T=10^{-4} - 10^{-5}$ level and specify theoretical predictions of SSF.

We want to emphasize in final remarks the significance of SSF detection which leads to the discovery of the Cosmological molecules. Cosmological molecules can provide an unique test to non-standard nuclear synthesis at high z . SSF can only help us in investigating Dark Ages epoch in the Early Universe ($300 > z > 10$). SSF detection at $z=20-30$ may give an important information about ionization history of the Universe. Finally, they will allow us to explore physical properties of Dark Matter and Dark Energy.

6 Conclusion

Observational effects caused by interaction of primordial molecules with CMBR seem to be most promising in investigating of Dark Ages epoch of the Early Universe and ionization history of the Universe. Strategy and concept of the experiment are given. Simulation of the experiment in an atmospheric transparency window at 3 mm with MSRT equipped with a 7x4 beam cryo-microbolometer array gives us the expected sensitivity of 50-55 μK in the differential CMBR maps near NCP with angular resolution $6'-7'$ ($l=1200-1500$) and frequency resolution $\Delta\nu/\nu=2\%$. The expected integral sensitivity in the experiment is $\Delta T/T=2\cdot 10^{-5}$ which is near to optimistic estimates of SSF caused by molecules HeH^+ at $z=20-30$. Simulation shows that SSF may be recognized in the angular power spectrum when S/N in single frequency CMBR maps is as small as 1.17 for a white noise. Such an experiment will give us a possibility to set upper limits in SSF observations in MM band and prepare future SSF experiments.

References

- [1] Ali, L. et al. Planar Antenna-Coupled Transition-Edge Hot Electron Microbolometer, 2003, IEEE TRANS. AS, 13.
- [2] Basu, K., Hernandez-Montenegro, C., Sunyaev, R., 2004, A&A, 416, 447-466.
- [3] Benford, D. et al., A planar two-dimensional superconducting bolometer array for the Green bank Telescope, 2004, SPIE, 5498, 208-218.
- [4] Bennet, C.L, Hill R.S., G.Hinshaw et al., 2004, ApJ, in press.
- [5] Crill B.P. et al., 2002, Ap J, v.676.

- [6] de Bernardis, P., V.Dubrovich et al., 1993, A&A, 269, issue 1/2, 1-6.
- [7] de Bernardis et al., 2002, Ap.J., 564, 559.
- [8] Bond, J.R., Efstathiou, G., 1987, MNRAS, 226, 655.
- [9] Doroshkevich, A. G., Dubrovich, V. K., 2001, MNRAS, 328, 79.
- [10] Dubrovich, V.K., 1975, Soviet Astron. Letters, 1, 196.
- [11] Dubrovich, V.K., 1977, Astron. Letters, 3, 243.
- [12] Dubrovich, V.K., 1977/2, PhD thesis, St.Petersburg, Pulkovo.
- [13] Dubrovich, V.K, 1982, Izvestia SAO, 15, 21.
- [14] Dubrovich, V.K., Lipovka, A.A., 1995, A&A, 296,301.
- [15] Dubrovich,V.K., Stolyarov, V.A., 1995, A&A, 302, 635.
- [16] Dubrovich, V.K., 1997, A&A, 324, 27.
- [17] Dubrovich, V.K., Bajkova, A.T., 2003, Astron. Lett., 29, 567-572.
- [18] Dubrovich, V.K.,Bajkova, A.T., Khaikin, V.B. In Proceedings of the International Conference "Exploring the Cosmic Frontier: Astrophysical Instruments for the 21 st. Century", Berlin, Germany, 2004.
- [19] Dubrovich, V.K., Shakhvorostova, N.N., 2004, Astron. Lett., 30,509.
- [20] Dubrovich, V.K., Grachev, S.I. 2004, Astron. Lett., 30, 657.
- [21] Goldin, A., Bock, J. et al., Design of broadband filters and antennas for SAMBA, 2003, in Proceed. Of SPIE, 4855, 163-171.
- [22] Fixsen, D.J., Mother, J.C., 2002, ApJ, 581, 817.
- [23] Fixsen et al., 2004, ApJ, 612, 86-95.
- [24] Gorski,K.M., 1997, In Proceedings of the XXXI-st Recontres de Marion Astrophysics Meeting, 77.
- [25] Granet, C.,James, G.L., Bolton, R., Moorey, G. 2004, Antennas and Propagation, IEEE Trans., 52, 848 - 854.
- [26] Fowler,J. The Atacama Cosmology Telescope Project, 2004, SPIE, 5498.
- [27] Gosachinskii, I.V., Dubrovich, V.K. et al., 2002, Astron. Rep., 46, 543-550.
- [28] Kasyanov, A., Khaikin, V., In Proceedings of 27 th ESA Antenna Technology Workshop on Innovative Periodic Antennas (WPP-22), Santiago de Copostela, Spain, March 9-11, 2004.
- [29] Khaikin, V., Yakovlev, S., Kazarinov A., Efimov, I., Volkov A., Valtaoja E. Convention on Radio Science, pp.84-87, Espoo, Finland, Oct.2002.

- [30] Khaikin, V., Yakovlev S., Kazarinov A., Karavaev, D., Rybakov, Yu. 2003, In Proceed. of 3-d ESA Workshop on MM-wave Technology and Applications, Espo, Finland, 425-430.
- [31] Khaikin, V., Luukanen A. 2003, In Proceed. of 3-d ESA Workshop on MM-wave Technology and Applications, pp.419-425, Espo, Finland.
- [32] Khaikin, V.B., Dubrovich, V.K. MM-wave radio telescope with multibeam focal plane array for SSF search. 2004, in Proceedings of IRMMW-2004, Karlsruhe, Germany.
- [33] Khaikin, V.B., Luukanen, A., Dubrovich, V.K., Instrumental and atmospheric noise in ground based MM-wave SSF experiment, 2005, G&C, 11.
- [34] Khaikin, V.B. Simulation of antenna characteristics of mm-wave radio telescopes with multibeam FPA. In Proceedings of 28 th ESA Antenna Workshop on Space Antenna Systems and Technologies, Noordwijk, The Netherlands, May, 2005.
- [35] Khaikin, V.B., Chung M-H., Radzikhovskiy V.N., Kuzmin S.E., Kaplya S.V., Simulated characteristics of 14 m MM-wave TRA0 telescope with multibeam FPA at 85-115 GHz, 2005, G&C, 11.
- [36] Khaikin, V.B., Radzikhovskiy, V.N. , Kuzmin S.E., Shlensin, S.V., Popenko, Chernobrovkin, R. Granet, C. Tightly packed multibeam FPA at 30-38 GHz. In Proceed. of 29 th ESA Antenna Conference, Noordwijk, The Netherlands, April, 2007.
- [37] Kogut A., Spergel, D.N., Barnes, C. et al., 2003, ApJS, 148, 161.
- [38] Lawrence, C.R., Gaier, T., Seiffert, M., Millimeter-Wave MMIC Cameras and the QUIET Experiment, 2004,. Proceedings of SPIE, 5498.
- [39] Lepp, S., Shull, J.M., 1984, ApJ, 280, 465.
- [40] Low, F.J., Beintema, D.A., Gautier, T.N., Gillett, et al. 1984. Ap. J. Lett. 278; L19-L22.
- [41] A.Luukanen, J.Pekola. Applied Physics Letters, v.82, pp.3970-3972, 2003.
- [42] Maoli, R., Melchiorri. F., Tosti, P. 1994, ApJ., 425, 372-381.
- [43] Maoli, R. et al., 1996, ApJ., 457, 1.
- [44] Majorova, E.K., Khaikin, V.B. Characteristics of radio telescopes with multielement microstrip focal plane arrays. Radiophysics, v.XLVIII, N2, pp.95-109, 2005.
- [45] Mather, J.C., Cheng, E.S. et al., ApJ, 420,439. 1994.
- [46] Mauskopf, P.D. B.K. Rownd, S.F. Edgington, V.V. Hristov, A. K. Mainzer, J.Glenn, A.E. Lange, J.J. Bock, and P. A. R Ade. Proc. Imaging at Radio through Submillimeter Wavelengths. 2000, ASP Conference Series, 217, p.115.

- [47] Miller, A.D. Proceedings of MG-9, World Scientific, Singapore, 2001.
- [48] Myers M. et al. Applied Physics Letters, 86,114103, 2005.
- [49] Page, L. Millimeter-submillimeter wavelength filter system.1994, Applied Optics.v.33, N1.
- [50] Page, L. et al. astro-ph/0603450, 2006.
- [51] Palla,F et al.,1995, ApJ,451,44.
- [52] Parijskij, Y.N., Korolkov, D.V. Experiment "Cold" , Sov. Sci. Rev. E Astrophys. Space Phys., Vol. 5, 1986, pp. 39-179.
- [53] Parijskij, Yu.N. Bursov, N.N. Berlin, A.B. Balanovskij, A.A. Khaikin, V.B. Majorova, E.K. Mingaliev, M.G. Nizhelskij, N.A. Pylypenko, O.M. Tsibulev, P.A. Verkhodanov, O.V. Zhekanis, G.V. Zverev, Yu.K. RATAN-600 new zenith field survey and CMB problems. Gravitation&Cosmology, 10(2004), pp.1-10.
- [54] Peacock,J.A.1999, Cosmological Physics, Cambridge Univ.Press, chap.18.
- [55] Peebles, P.J.E.1993, Principles of Physical Cosmology, Princeton Univ.Press, chap.21.
- [56] Puy, D. et al., 1993, A&A, 267, 337.
- [57] Readhead, A. et al. 2004, ApJ, 609, 418.
- [58] Rubino-Martin,J.A, Mernandez-Monteaagudo, C. and Sunyaev, R.A., 2005, astro-ph/0502571
- [59] Ruhl, J.E. et al. The South Pole Telescope. 2004, Proc. SPIE, 5498.
- [60] Spergel, D.N., Verde, L., Peris, H.V. et al., 2003, ApJS, 148, 175.
- [61] Spergel, D.N. et al., 2006, astro-ph/0603449.
- [62] Stancil, P.D., Lepp, S., Dalgarno, A., 1996, ApJ, 458, 401S.
- [63] Sunyaev, R.A., Zel'dovich Ya.B., 1970. Ap&SS, 7, 3-19.
- [64] Sahni, V.,Starobinsky, A., 2000, Int.J.Mod.Phys., 9, 373-444.
- [65] Varshalovich, D., Khersonskii, V., Suyae, R., 1981, Astrophysics, 17, 273.
- [66] Vdovin, V.F. Radiophysics, 2005, 48, 876.
- [67] Wyithe,J., Loeb, A., 2003, ApJ, 322, 597.
- [68] Wollack, E. J., Jarosik, N., Netterfield et al.,1 994, Astrophys. Lett. Commun., 35, 217.
- [69] Zel'dovich, Ya.B., Novikov, I.D., Structure and evolution of the Universe, Moscow, Nauka, 1975.
- [70] Zel'dovich, Ya.B., 1978, Sov.Astron.Lett., 4, 165.